Coexistence of spin canting and metamagnetism in a one-dimensional Mn(II) compound bridged by alternating double end-to-end and double end-on azido ligands and the analog co(II) compound

Benamara, N.; Setifi, Z.; Yang, C.I.; Bernès, S.; Geiger, D.K.; Kürkçüoğlu, G.S.; ... ; Reedijk, J.

Note: To cite this publication please use the final published version (if applicable).

Coexistence of Spin Canting and Metamagnetism in a One-Dimensional Mn(II) Compound Bridged by Alternating Double End-to-End and Double End-On Azido Ligands and the Analog Co(II) Co…

Article *in* Magnetochemistry · April 2021

DOI: 10.3390/magnetochemistry7040050

8 authors, including:

Nesrine Benamara
Institut de Physique et Chimie des Matériaux de Strasbourg
3 PUBLICATIONS   **2** CITATIONS

SEE PROFILE

Zouaoui Setifi
Université 20 août 1955-Skikda
107 PUBLICATIONS   **223** CITATIONS

SEE PROFILE

David K Geiger
State University of New York College at Geneseo
168 PUBLICATIONS   **2,444** CITATIONS

SEE PROFILE

Güneş Süheyla Kürkçüoğlu
Eskisehir Osmangazi University
72 PUBLICATIONS   **529** CITATIONS

SEE PROFILE

Some of the authors of this publication are also working on these related projects:

Project   platinum coordination complexes as Universal Linkage System ULS View project

Project   oxidative coupling of 2,6-dimethylphenol View project

Article

Coexistence of Spin Canting and Metamagnetism in a One-Dimensional Mn(II) Compound Bridged by Alternating Double End-to-End and Double End-On Azido Ligands and the Analog Co(II) Compound †

Nesrine Benamara [1], Zouaoui Setifi [1,2] , Chen-I Yang [3,*], Sylvain Bernès [4] , David K. Geiger [5] , Güneş Süheyla Kürkçüoğlu [6] , Fatima Setifi [1,*] and Jan Reedijk [7,*]

[1] Laboratoire de Chimie, Ingénierie Moléculaire et Nanostructures (LCIMN), Université Ferhat Abbas Sétif 1, Sétif 19000, Algeria; nes_benamara@yahoo.com (N.B.); setifi_zouaoui@yahoo.fr (Z.S.)
[2] Département de Technologie, Faculté de Technologie, Université 20 Août 1955-Skikda, Skikda 21000, Algeria
[3] Department of Chemistry, Tunghai University, Taichung 407, Taiwan
[4] Instituto de Física, Benemérita Universidad Autónoma de Puebla, 72570 Puebla, Mexico; sylvain_bernes@hotmail.com
[5] Department of Chemistry, SUNY-College at Geneseo, Geneseo, NY 14454, USA; geiger@geneseo.edu
[6] Department of Physics, Eskişehir Osmangazi University, 26040 Eskişehir, Turkey; gkurkcuo@ogu.edu.tr
[7] Leiden Institute of Chemistry, Leiden University, P.O. Box 9502, 2300 RA Leiden, The Netherlands
* Correspondence: ciyang@thu.edu.tw (C.-I.Y.); fat_setifi@yahoo.fr (F.S.); reedijk@chem.leidenuniv.nl (J.R.)
† Dedicated to the memory of Prof. Peter Day, who passed away in May 2020.

Abstract: Two new compounds of general formula [M(N$_3$)$_2$(dmbpy)] in which dmbpy = 5,5′-dimethyl-2,2′-bipyridine, and M = Mn(II) or Co(II), have been solvothermally synthesized and characterized structurally and magnetically. The structures consist of zig-zag polymeric chains with alternating bis-μ(azide-N1)$_2$M and bis-μ(azide-N1,N3)$_2$M units in which the cis-octahedrally based coordination geometry is completed by the N,N'-chelating ligand dmbpy. The molecular structures are basically the same for each metal. The Mn(II) compound has a slightly different packing mode compared to the Co(II) compound, resulting from their different space groups. Interestingly, relatively weak interchain interactions are present in both compounds and this originates from π–π stacking between the dmbpy rings. The magnetic properties of both compounds have been investigated down to 2 K. The measurements indicate that the manganese compound shows spin-canted antiferromagnetic ordering with a Néel temperature of T_N = 3.4 K and further, a field-induced magnetic transition of metamagnetism at temperatures below the T_N. This finding affords the first example of an 1D Mn(II) compound with alternating double end-on (EO) and double end-to-end (EE) azido-bridged ligands, showing the coexistence of spin canting and metamagnetism. The cobalt compound shows a weak ferromagnetism resulting from a spin-canted antiferromagnetism and long-range magnetic ordering with a critical temperature, T_C = 16.2 K.

Keywords: azide; chain compounds; ferromagnetism; antiferromagnetism; metamagnetism; spin canting

1. Introduction

Coordination compounds with azide ligand have been studied for decades, not only for their potential use as detonation agents or explosives [1–5], but also because of the intrinsic properties of N$_3$$^-$ as a "pseudo halogen" [6,7] and as a subject of magnetism [8]. Many studies of stable azide coordination compounds have been reported, and the Cambridge Structural Database (2020 release) contains over 5000 items having at least one coordinated azide ligand [9].

Azide ligands can bind monodentately to metal ions in an end-on mode (N1), or they can bridge between two or more metal ions. Bridging azide between two metals

can take place using one terminal nitrogen only (i.e., N1,N1, known as *end-on* mode, abbreviated in this manuscript as EO), or two terminal nitrogens (i.e., N1,N3 or *end-to-end* mode, abbreviated as EE). In the bridging mode, dinuclear compounds can be formed, like in M(azide)$_2$M species [10], as depicted in Figure 1, but also polynuclear compounds, including polymeric linear or zig-zag species of formula ···(azide)$_2$M(azide)$_2$M(azide)$_2$ ···. Mixed species with both terminal (non-bridging) and bridging azide are known in the literature [8,11–14], but are not so common.

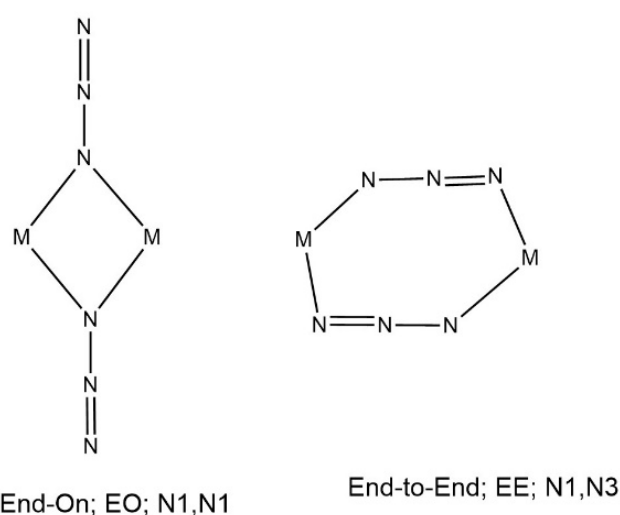End-On; EO; N1,N1   End-to-End; EE; N1,N3

Figure 1. Schematic representation of the binding modes for bridging azido ligands between two metal ions M.

In earlier reports from our laboratories, we have given attention to metal–azide compounds as bridging ligands for dinuclear compounds, or higher aggregates up to 2D networks [15–18] and we have found both ferromagnetic and antiferromagnetic cases. The ferromagnetic cases are only known for the EO azido-bridged compounds. It appears that the choice of the non-bridging co-ligands plays a major role on the formation of specific compounds and structures, and also whether EO, EE or a combination is found. As the azido ligands are rather small or narrow, to generate relative stable coordination spheres around the metal, the co-ligands should be rather bulky, as shown from the literature examples above.

In the present paper, we report on two new compounds that have alternating modes (EE and EO) of bridging azide, forming zig-zag chains in the solid state. The compounds have interesting magnetic properties and these are studied in detail using magnetic susceptibility and magnetization studies at low-temperature (down to 2 K). We feel that the study is relevant in the search for potentially cheap, stable and useful new magnets.

2. Results and Discussion

2.1. Synthetic Efforts

Both title compounds were easily synthesized by the hydrothermal method and the synthesis was found to be reproducible. Despite several attempts, no pure crystalline materials could be isolated for the similar Fe(II) compound. In most attempts, two crystalline forms could be obtained, one isomorphous with the Mn(II) compound and the other isomorphous with the Co(II) compound. Therefore, this compound was not considered suitable for the study of the magnetic properties. In contrast, pure bulk samples for the Mn(II) and Co(II) compounds were available, as evidenced by powder diffraction data, which are consistent with patterns simulated from single-crystal data (Figure S1).

2.2. Characterization of the Compounds by IR and Elemental Analysis

Both compounds display very similar infrared spectra (Figure S2), where bands resembling the free dmbpy ligand are easily recognized. Most characteristic is the broad strong band (doublet) near 2087 cm^{-1}, typical for the coordinated bridged azide ligand [19–21]. The elemental analyses of both compounds are in full agreement with the values calculated, and with the 3D structures presented below, indicating that no secondary phases were obtained with the used synthetic methodology.

2.3. Structure Description of the Compounds

Single crystal structures were determined for both synthesized compounds (**1** and **2**) [M(N$_3$)$_2$(dmbpy)], with M = Mn(II) and Co(II) and dmbpy = 5,5'-dimethyl-2,2'-bipyridine (C$_{12}$H$_{12}$N$_2$). The Mn(II) compound (**1**) crystallizes in space group P-1, while the Co(II) compound (**2**) crystallizes in space group $P2_1/c$. Even though the space groups are different, both compounds share the same molecular structure (see Figure 2 for the Mn(II) compound). The metal center is coordinated by the bidentate dmbpy ligand and two azido anions. Since both pseudohalides, azido N$_3^-$ ligands, bridge between symmetry-related metal centers in the crystal, a one-dimensional polymeric structure is formed, in which each azido anion has a different function: two anions N3/N4/N5 form a centrosymmetric double-bridge, with the μ-1,1 mode of coordination (EO). Two other anions, N6/N7/N8, also form a centrosymmetric double-bridge, but this time with the μ-1,3 coordination mode (EE).

Figure 2. Part of the polymeric structure of *catena*-poly-[Mn(N$_3$)$_2$(dmbpy)] with displacement ellipsoids for non-H atoms at the 30% probability level. Mn and N atoms belonging to the asymmetric unit are labelled, as well as symmetry-related metallic centers along the chain. Symmetry codes: (**i**) 1 − x, 1 − y, 1 − z; (**ii**) −1 + x, y, z; (**iii**) 2 − x, 1 − y, 1 − z; (**iv**) 1 + x, y, z.

Both coordination modes alternate along the zig-zag polymeric chains, which run parallel to the a-axis regardless of the crystal system, triclinic (*M* = Mn) or monoclinic (*M* = Co). Relevant coordination bond lengths and angles are given in Table 1. The trend of the well-known smaller ionic radii going from Mn(II) to Co(II) is clearly visible.

Table 1. Selected bond lengths (in Å) and angles (deg.) for both compounds.

Compounds	[Mn(N$_3$)$_2$(dmbpy)]	[Co(N$_3$)$_2$(dmbpy)]
M–N1	2.272(3)	2.115(5)
M–N2	2.256(4)	2.133(5)
M–N3	2.215(4)	2.144(5)
M–N3	2.222(3) [a]	2.198(6) [c]
M–N6	2.208(3)	2.140(6)
M–N8	2.263(3) [b]	2.204(6) [d]
N1–M–N2	72.26(11)	76.7(2)
N3–M–N6	99.50(15)	95.2(2)
N1–M–N3	95.59(12) [a]	94.1(2)
N1–M–N6	162.97(15)	170.6(2)
N2–M–N6	91.83(14)	94.3(2)
N3–M–N3	79.08(12) [a]	78.6(2) [c]
N6–M–N8	90.56(12) [b]	88.8(2) [d]
N2–M–N3	168.67(12)	167.5(2)

Symmetry for the last N atom: [a] $1 - x, 1 - y, 1 - z$; [b] $2 - x, 1 - y, 1 - z$; [c] $-x, -y, 1 - z$; [d] $1 - x, -y, 1 - z$.

Along the chain, long and short $M \cdots M$ separations alternate, 5.430(1) and 3.422(1) Å for M = Mn and 3.361(2) and 5.317(2) Å for M = Co. These distances are slightly shorter for the Co(II) compound as a result of the smaller ionic radii of the cations. The polynuclear zig-zag chains are packed efficiently in the crystal. With M = Mn, chains are parallel, and the dmbpy ligands of two neighboring chains are stacked in such a way that they interact with a rather short distance, 3.440 Å. For M = Co, the arrangement of chains in the crystal is slightly modified, because of the monoclinic cell symmetry. However, the relative position of two neighboring chains is essentially preserved, and the π–π interactions between the dmbpy ligands are even strengthened, with separations between ligand mean planes of 3.283 Å (Co). In Figure 3, both different packings are depicted.

In [Mn(N$_3$)$_2$(dmbpy)], the N–N bond lengths are symmetrical in the EE azido ligands but are asymmetric in the EO ligands. The bite angle exhibited by the dmbpy ligand (72.26(11)°) is the largest distortion in the geometry of the *cis*-octahedral coordination sphere. The four-membered Mn$_2$(EO-N$_3$)$_2$ ring is planar as a result of the inversion center. The eight-membered Mn$_2$(EE-N$_3$)$_2$ ring adopts a chair configuration. The dihedral angle δ, defined by the N6/Mn1/N8 plane and the (EE-N$_3$)$_2$ plane, is 9.69(3)° and Mn1 sits 0.266(7) Å out of the (EE-N$_3$)$_2$ plane. The Mn–azido–Mn torsion angle τ, defined by the dihedral angle between the mean planes of Mn1-N6-N7-N8 and Mn1-N8-N7-N6, is 20.3(6)°. Similarly, in [Co(N$_3$)$_2$(dmbpy)], the N–N bond lengths are approximately symmetrical in the EE azido ligands but are asymmetric in the EO ligands. The bite angle exhibited by the dmbpy ligand (76.7(2)°) is the largest distortion in the geometry of the *cis*-octahedral coordination sphere. The four-membered Co$_2$(EO-N$_3$)$_2$ ring is planar as a result of the inversion center. The eight-membered Co$_2$(EE-N$_3$)$_2$ ring adopts a chair configuration. The dihedral angle δ, defined by the N6/Co1/N8 plane and the (EE-N$_3$)$_2$ plane, is 25.2(4)°. Co1 sits 0.66(1) Å out of the (EE-N$_3$)$_2$ plane. The Co–azido–Co torsion angle τ, defined by the dihedral angle between the mean planes of Co1-N6-N7-N8 and Co1-N8-N7-N6, is 47.7(6)°.

The azide ligand is well known for its versatility in coordination behavior, as explained in the introduction. When involved in metal-to-metal bridges, coordination modes EO and EE are frequent; however, the EO mode is roughly ten times more common than the EE mode, based on a survey of the Cambridge Structural Database [9]. Toggling EO and EE modes along a 1D polymeric structure is rare, but not unprecedented (see Table S1). Indeed, quite similar azido-bridged structures have been described using other ancillary ligands and a variety of transition metals: Schiff bases and Mn(II) [22,23] pyridine derivatives and Mn(II) [24,25], Co(II), Ni(II) [14] or Zn(II) [21] amine/pyridine derivatives and Ni(II) [11,26,27], among others. The nearest structurally related compound is certainly [Mn(N$_3$)$_2$(2,2′-bipyridine)], which crystallizes in space group *P*-1, with unit–cell parameters

quite close to those of [Mn(N$_3$)$_2$(dmbpy)] [13,28] and in fact is even isostructural with the Fe(II) and Co(II) analogues [29].

Compounds based on azido-EE/EO double bridges are of interest in the field of magnetochemistry, because the type of interaction between magnetic centers is not unexpected. Therefore, it was decided to perform a detailed magnetic analysis down to very low temperatures. The results are described in the next section.
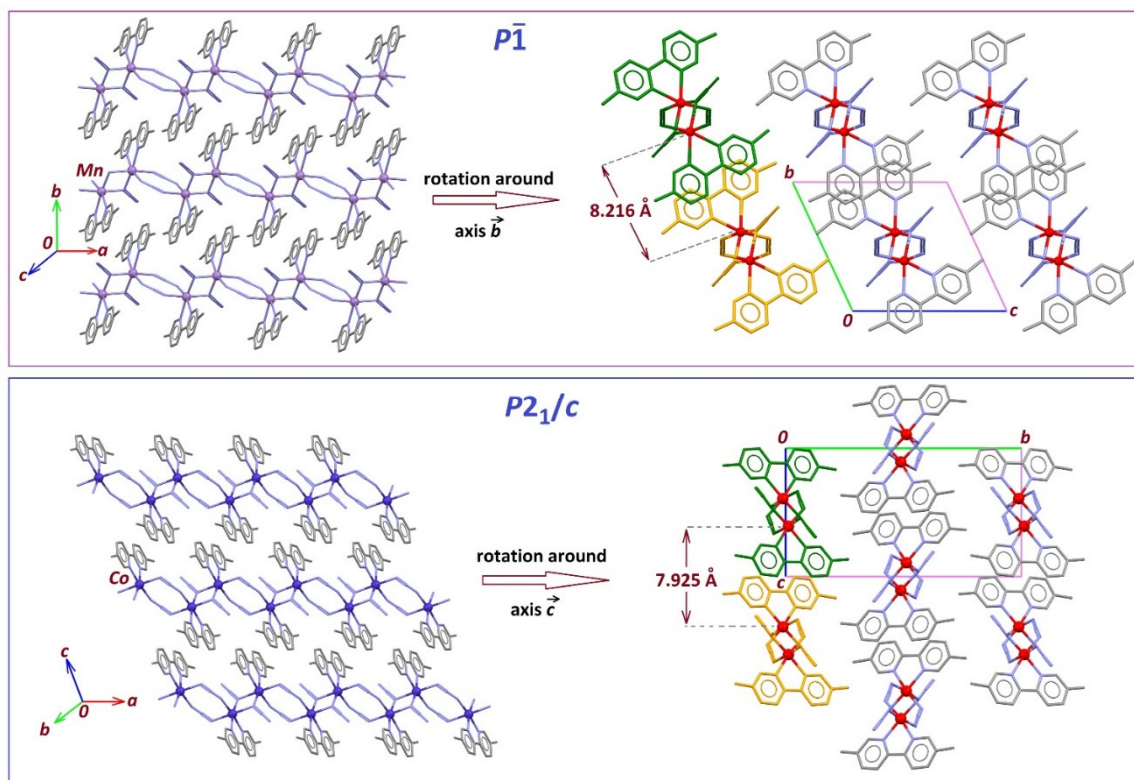

Figure 3. Projection of the packing structures for compounds **1** (top) and **2** (bottom). On the figures on the left side, crystal structures are viewed in a plane where 1D chains are parallel, emphasizing π–π interactions between aromatic rings. By rotation around a crystallographic axis, crystal structures are viewed down the polymerization direction (right side), showing the arrangement of the chains in the crystal. Green and gold parts are different parallel chains, and shortest interchain metal–metal (M–M) distances are quoted in both crystals. Closest M–M contacts are greater than 8.2 Å for **1** and greater than 7.9 Å for **2**.

2.4. Magnetic Properties

For compounds with two different azide binding modes, one can expect interesting magnetic properties, as metal–metal exchange can occur via two different pathways. It is clear that the EE bridges, with their large metal⋯metal separations, will always be involved in antiferromagnetic coupling (AF) [8]. The AF interaction is increased if the eight-membered metallacycle M(N$_3$)$_2M'$ is essentially planar. In contrast, EO bridges may promote ferromagnetism (F), provided the M–N–M angle is less than 108° [8]. Regarding the AF component, the triclinic compound (M = Mn) is expected to display a similar or even greater AF interaction than the monoclinic compounds (M = Co), since the former has an EE bridge almost flat, while the bridges in the latter have a butterfly conformation: the dihedral angle δ between the (N$_3$)$_2$ mean plane and the plane formed by M and the bonded N$_{azido}$ atoms is δ = 9.69(3)° for M = Mn, and δ = 25.2(4)° for M = Co. Regarding the F component, both compounds fulfil the requirement for potentially having $J > 0$. The observed angles at EO bridges are 100.92(12) and 101.4(2)° for M = Mn, Co, respectively.

On the other hand, the six-coordinated metal ions used in this work are located in a slightly distorted octahedral ligand field, and their electronic configurations allow

for either a low, or a high-spin state, depending on the crystal field splitting Δ_o for $3d$ orbitals. In the present case, the spectrochemical series indicates that $N_3{}^-$ is a relatively weak ligand, while dmbpy is a relatively strong ligand. There is thus a competition between π-donation and π-backdonation in the coordination sphere, which makes the ground spin state not straightforward to anticipate. However, crystal structures are helpful in this regard, because Δ_o is also related to the strength of any Jahn–Teller (JT) effect in a crystal field with octahedral symmetry. Assuming a small tetragonal distortion, a symmetry measure accounting for the octahedral character of the field can be computed as $S(O_h) = 5.39\Delta^2 - 0.33|\Delta|$, where Δ is the difference between the largest and the shortest coordination bond lengths. Structures with $S(O_h) < 4.42$ are closer to the octahedron than to the trigonal prism geometry [30].

For the Mn(II) compound, $S_{Mn}(O_h) \sim 10^{-3}$, reflecting a very small departure from the ideal O_h symmetry, which, in turn, confirms that the JT distortion indeed is not present, consistent with a high-spin configuration. For the Co(II) compound, the JT distortion is much more noticeable, with $S_{Co}(O_h) \sim 13.10^{-3}$, in line with weak JT distortions, as expected for high-spin d^7 ions; (in particular, a low-spin configuration for Co^{2+}, with an odd number of electrons in the e_g orbitals would give rise to a strong JT effect, associated to a symmetry measure of the field $S(O_h) \gg 10^{-2}$).

It is evident that the crystal structures for the newly synthesized compounds allow one to predict the ground spin state for each one, $S = 5/2$ and $S = 3/2$ for M = Mn(II) and Co(II), respectively. On the other hand, both antiferromagnetic and ferromagnetic interactions should alternate along the 1D chains. Structural features obtained from X-ray structures are, however, not enough to confidently assess the balance between F and AF interactions in these materials, and a comprehensive experimental study of magnetic susceptibility was thus warranted.

Mn Compound (1). The temperature dependences of χ_M and $\chi_M T$ are depicted in Figure 4. At 300 K, the $\chi_M T$ value per Mn(II) ion of compound **1** is 3.80 cm^3 mol^{-1} K, which is lower than the spin-only value of 4.38 cm^3 mol^{-1} K expected for a magnetically isolated octahedral high-spin Mn(II) ion with $g = 2.00$. Upon cooling, the $\chi_M T$ values decrease gradually and show the cusp around 3.5 K, with a $\chi_M T$ value of 0.317 cm^3 mol^{-1} K at 3.5 K, decreasing to a value of 0.194 cm^3 mol^{-1} K at 2.0 K. The monotonic $\chi_M T$ decrease at a high temperature is indicative of the existence of antiferromagnetic coupling. Upon cooling, the χ_M increases smoothly from 0.013 cm^3 mol^{-1} at 300 K to reach a plateau of 0.035 cm^3 mol^{-1} at about 14.6 K, and then increases rapidly, reaching a maximum of 0.098 cm^3 mol^{-1} at 2.5 K, before a slight decrease to a value of 0.096 cm^3 mol^{-1} at 2.0 K. The sharp increase in χ_M at a low temperature is likely due to a small amount of paramagnetic impurities, e.g., at crystal edges and vacancies along the plane, as is known for related cases [31,32], or perhaps to some features of uncompensated spin. The temperature dependence of $1/\chi_M$ at temperatures above 110 K can be fitted by the Curie–Weiss law with $C = 4.64(4)$ cm^3 mol^{-1} K and $\theta = -64.7(6)$ K (Figure S3). The negative Weiss constant suggests the presence of overall antiferromagnetic coupling between the adjacent Mn(II) ions.

To try to obtain intrachain magnetic couplings between Mn(II) ions through the double EO–N$_3$ and double EE–N$_3$ bridges, the magnetic susceptibility of compound **1** was fitted using the expression proposed by Cortés [13,28], for alternating chains of classical spins on the Hamiltonian $H = -J_1\Sigma S_{2i}S_{2i+1} - J_2\Sigma S_{2i+1}S_{2i+2}$.

$$\chi_M = [Ng^2\beta^2 S(S + 1)/3kT][(1 + u_1 + u_2 + u_1 u_2)/(1 - u_1 u_2)] \tag{1}$$

where $u_i = \coth[J_i S(S + 1)/kT] - kT/[J_i S(S + 1)]$ ($i = 1$ and 2) with $S = 5/2$, J_1 and J_2 are the F and AF exchange constants through double EO–N$_3$ and double EE–N$_3$ superexchange pathways, respectively.
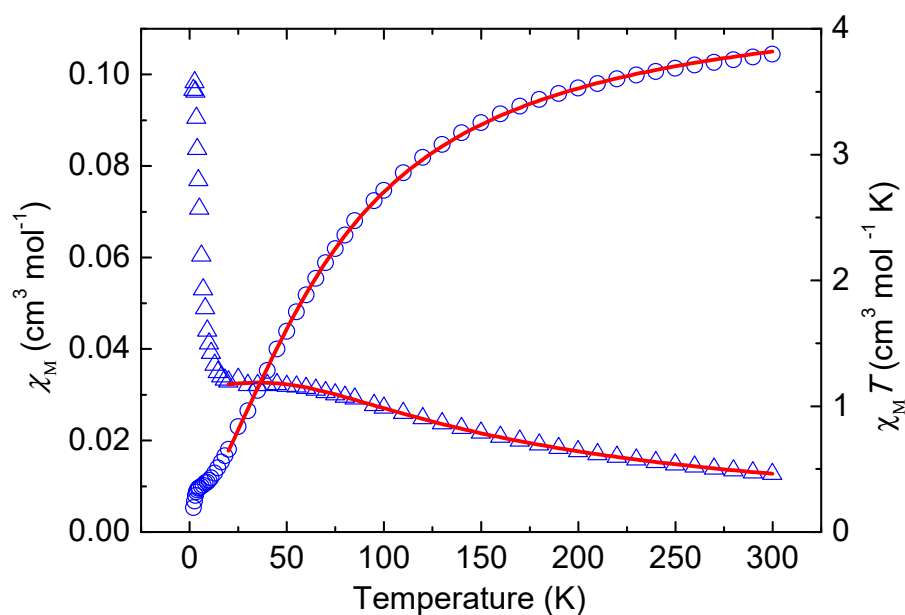
Figure 4. The temperature dependences of χ_M (triangles) and $\chi_M T$(circles) of compound **1**. The solid line represents the best fit given in the text.

The data above 20 K were fitted and the best fit to experimental data led to J_1= 2.87(7) cm^{-1}, and J_2 = −11.3(9) cm^{-1} with a fixed g = 2.0. The J_1 and J_2 parameters are consistent with the reported results for related compounds. As in the earlier theoretical and experimental studies, the magnetic couplings between Mn(II) ions via the double EO–N$_3$ bridge were usually ferromagnetic due to small Mn–N–Mn angles which would lead the orthogonality of the magnetic orbitals of the adjacent Mn(II) centers. In contrast, the antiferromagnetic couplings were usually dominated via the EE–N$_3$ bridge due to the well overlap of magnetic orbitals of the adjacent Mn(II) centers. The ferromagnetic interaction decreases with the increasing Mn–N$_{azide}$–Mn angle, while the antferromagnetic couplings via double EE–N$_3$ bridges were dependent on the δ angle, the dihedral angle between the N$_{azide}$–Mn–N$_{azide}$ plane and the plane defined by the two azido bridges, the magnetic coupling decreases with the increasing δ angles [13]. The obtained magnetic coupling of two Mn(II) ions is ferromagnetic for a double EO–N$_3$ bridging with a small Mn–N$_{azide}$–Mn angle of 100.92(12)°, and is antiferromagnetic for a double EE–N$_3$ bridging with a small δ angle, 9.69(3)°, which are consistent with the reported results for related compounds [13,22,23,33–38]. In Table S1, a detailed overview of the literature is given with structural details and J values for a variety of Mn compounds, including the present two new compounds.

Furthermore, the temperature dependences of $\chi_M T$ for compound **1** under 100 Oe were also collected (see Figure S4), showing similar behavior to that under 1000 Oe except for that in the low-temperature range, in which the $\chi_M T$ value slightly increases with decreasing temperature below 6.0 K to a maximum of 0.381 cm^3 mol^{-1} K at 4.5 K and then sharply decreases to 0.076 cm^3 mol^{-1} K at 2.0 K. This suggests that a possible mechanism involving weak ferromagnetic correlations is operative within compound **1** below 6.0 K and the final decrease may be due to antiferromagnetic interactions between the chains and/or saturation effects. These weak ferromagnetic correlations can be attributed to spin canting, i.e., the antiferromagnetically coupled local spins within the –Mn–(EE-N$_3$)$_2$–Mn–EO-N$_3$)$_2$–chains are not perfectly antiparallel, but are canted with respect to each other, resulting in uncompensated residual spins [13,22,23,33–37].

To further characterize the low-temperature magnetic behavior of compound **1**, ZFC/FC magnetization measurements under a field of 10 Oe were carried out. As shown in Figure S5, the ZFC/FC magnetizations were found to be non-bifurcated and show a sharp maximum at 3.4 K, suggesting the occurrence of antiferromagnetic ordering. The

temperature dependence of the AC susceptibility of compound **1** was also measured at H_{dc} = 0 Oe and H_{ac} = 3.5 Oe at different frequencies (Figure S6), which shows the sharp frequency-independent value of the χ_M' signals with the peak maximum at 3.4 K. The absence of χ_M'' signals confirms the onset of antiferromagnetic ordering with a conventional T_N = 3.4 K and implies the existence of a magnetic phase transition.

The isothermal field dependence data of the magnetization of compound **1** was collected at 1.8 K (Figure 5), in which the magnetization shows a sigmoidal shape with an abrupt increase at a field above ~0.3 kOe to reach a value of 0.36 $N\beta$ at 70 kOe. This sigmoidal magnetization clearly indicates a field-induced magnetic transition of metamagnetic nature [39–41]. In this metamagnetic transition, the net moments of spin-canting Mn–N$_3$ chains aligned antiparallel under a weak applied field by weak interchain antiferromagnetic interactions are overcome by a stronger external field and result in the state transition from antiferromagnetic (AF) to paramagnetic (P). The critical field of magnetic transition, H_C, at 1.8 K, was estimated to be about 0.48 kOe as determined by dM/dH (Figure 5, inset). The M value of 0.36 $N\beta$ at 70 kOe is far below the expected saturation value of 5.0 $N\beta$ for an isotropic high-spin Mn(II) system, confirming the antiferromagnetic nature of **1**. Moreover, at 1.8 K, a small butterfly-shaped magnetic hysteresis loop was obtained, indicating a soft magnetic behavior (see Figure S7). The spin canting angle was estimated to be about α = 0.30°, based on the equation $\sin(\alpha) = M_R/M_S$ (M_R = 0.026 $N\beta$; obtained by extrapolating the high-field linear part of the magnetization curve at 1.8 K to zero field, and M_S = 5.0 $N\beta$) [42–45].
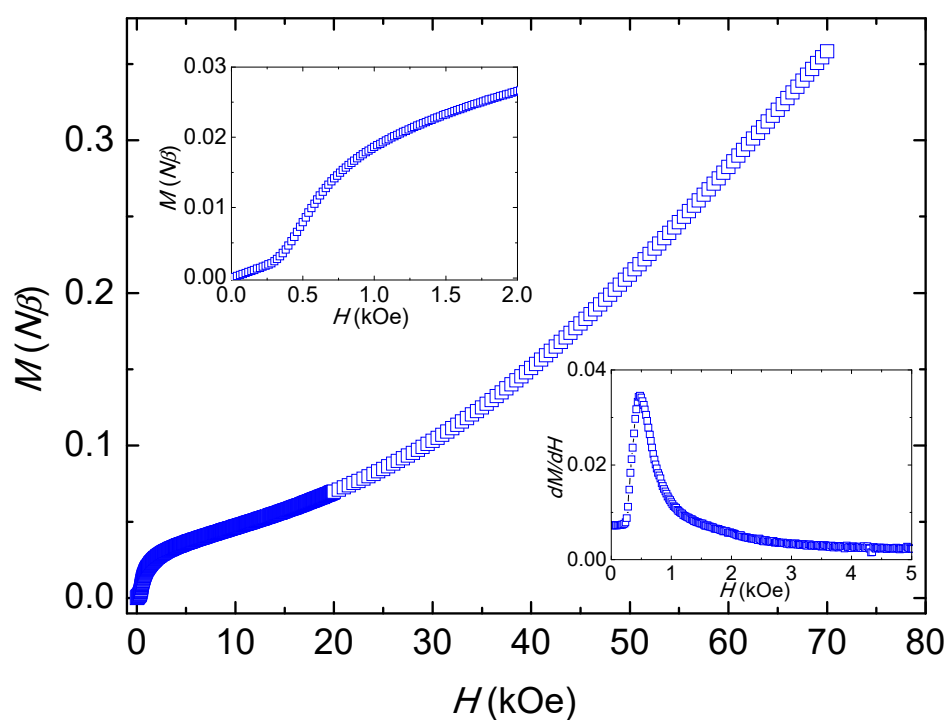

Figure 5. Isothermal magnetization of compound **1** at 1.8 K. The insets give the low field range and the derivative of M vs. H.

Generally speaking, spin canting can arise from two contributions: (i) the presence of an antisymmetric exchange Dzyaloshinsky−Moriya interaction [46] and (ii) the existence of single-ion magnetic anisotropy [47–52]. The presence of an inversion center between adjacent spin centers can result in the disappearance of the antisymmetric exchange. Hence, the lack of antisymmetric exchange in compound **1** would be expected, due to the existence of a crystallographic inversion center between the Mn(II) ions (see symmetry codes in caption of Figure 2). However, the Mn1 center in **1** displays a distorted octahedral geometry due to the small bite angle of 72.26(11)° of the dmbpy chelating ligand. Such distorted

octahedral geometries were reported as originating from the weak single-ion anisotropy of the high-spin Mn(II) site [53–57]. Therefore, it is assumed that the spin-canted antiferromagnetism in **1** can be attributed to weak single-ion magnetic anisotropy by a distorted metal coordination environment at low temperature. Similar spin canting behavior has been observed in a few other Mn(II) compounds containing chains of alternating double EO and double EE bridging modes of azides [34,58].

The field-induced magnetic phase transition for compound **1** was further investigated by the measurements of various fields of the FC magnetic susceptibilities, $\chi_M(T)$, and the field dependence of the magnetizations, $M(H)$, at different temperatures. As shown in Figure S8, the maximum of $\chi_M(T)$ shifts to lower temperatures with increasing applied field, until the $\chi_M(T)$ reaches a plateau at a field larger than 600 Oe, confirming that the weak interchain antiferromagnetic interaction is overcome by a stronger external field. As shown in Figure S9, at 2.0 K, the stepwise $M(H)$ curve clearly indicates a field-induced magnetic transition from AF to P. This stepwise magnetization becomes less pronounced with increasing temperature, and the differentials of these curves show peaks that shift to lower fields with increasing temperature (see Figure S10), indicating the phase transitions of metamagnetism.

Combining $M(H)$, FCM and the frequency-independent χ_M' data, the magnetic phase (T, H) diagram has been plotted in Figure 6. The value of H_C decreases with increasing temperature and finally disappears at about 3.4 K. The solid line of $H_C(T)$ in Figure 6, on an analysis of the M–H curves, signifies a typical magnetic transition from AF to P corresponding to metamagnetic materials.
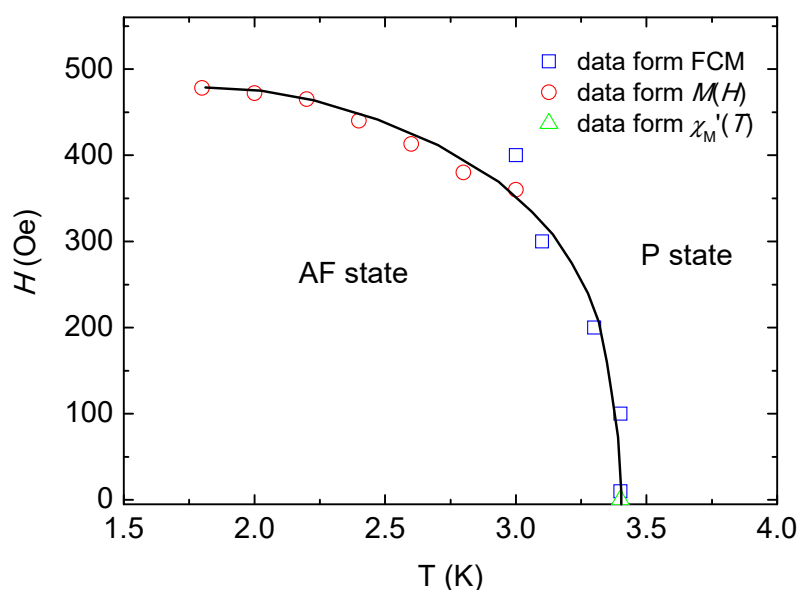

Figure 6. Magnetic phase (T, H) diagram for **1**, build up using the location of the maximum of χ_M vs. T data (open blue square), location of the maximum from dM/dH vs. H data (open red circle) and AC data (open green triangle); the solid line is a guide.

Co compound (2). The temperature dependences of χ_M and $\chi_M T$ of compound **2** are shown in Figure S11 and Figure 7, respectively. As the temperature decreases from 300 K, the χ_M value increases smoothly, reaching a rounded maximum of 0.021 cm³ mol⁻¹ at about 70 K, and then decreases slightly reaching a value of 0.015 cm³ mol⁻¹ at 20 K. Upon further cooling, the χ_M value increases rapidly to a sharp maximum of 0.017 cm³ mol⁻¹ at 12.8 K, after slightly decreasing, χ_M value increases again to 0.017 cm³ mol⁻¹ at 2.0 K. The temperature dependence of $1/\chi_M$ at temperatures above 100 K has been fitted by the Curie–Weiss law with a Curie constant C = 4.85 cm³ mol⁻¹ K and a Weiss constant θ = −130.5 K (see Figure S12).
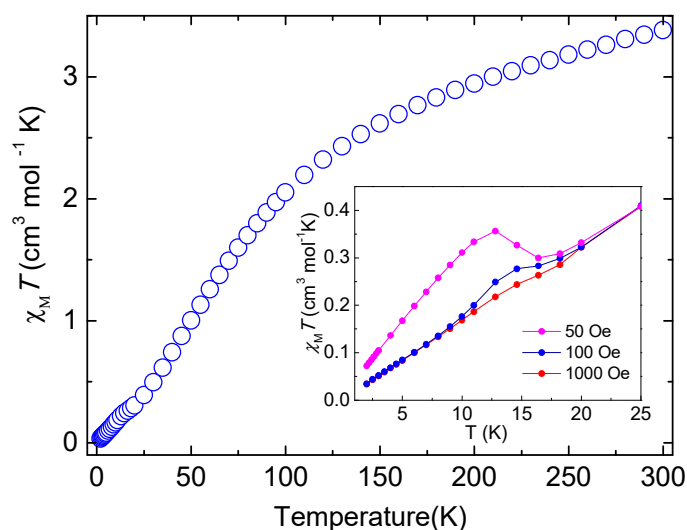
Figure 7. Plot of χ_MT vs. T of compound **2** in an applied field of 1 kOe from 2 to 300 K. The insets give the χ_MT vs. T at low temperature measured under the indicated external fields.

The large negative Weiss constant suggests the presence of strong spin-orbital coupling and/or overall antiferromagnetic interactions between the adjacent Co(II) ions. As shown in Figure 7, at 300 K, the $\chi_M T$ value per Co(II) of compound **2** is 3.38 cm^3 mol^{-1} K, which is larger than the spin-only value of 1.87 cm^3 mol^{-1} K for a magnetically isolated octahedral Co(II) ion ($S = {}^3/_2$), with g = 2.00. Upon cooling, the value of $\chi_M T$ decreases monotonically to attain a local minimum value of 0.299 cm^3 mol^{-1} K at 18.2 K, which is indicative of the existence of antiferromagnetic coupling. After a very small increase to a maximum value of 0.277 cm^3 mol^{-1} K at 14.6 K, the $\chi_M T$ value decreases again with further cooling to 2.0 K. The increase in $\chi_M T$ below 18.2 K is field-dependent, as shown in the inset of Figure 7; this suggests that a mechanism of weak ferromagnetic correlations due to spin canting antiferromagnetism is operative within compound **2**. The final decrease in $\chi_M T$ value may be attributed to antiferromagnetic interactions between the chain and/or saturation effects. Similar to the observations in compound **1**, the lack of antisymmetric magnetic interactions in compound **2** would be expected because of the presence of inversion centers in the $P2_1/c$ crystal structure. Thus, the spin canting of compound **2** originates from the single-ion anisotropy of the Co(II) ion, which is in agreement with the reported Co(II) spin canting compounds containing the same bridging mode of azide [59–61].

In order to substantiate the low-temperature magnetic properties of compound **2**, ZFC/FC magnetization studies were carried out at 50 Oe. As shown in Figure 8, upon cooling, both ZFC and FC magnetizations increase abruptly at temperatures below 18 K and a divergence between ZFC/FC below 16.2 K is observed, suggesting the occurrence of magnetic ordering for the formation of an ordered state and the existence of an uncompensated moment below the critical temperature of Tc = 16.2 K. Upon cooling, both ZFC and FC magnetizations increase again below 5.0 K, which may be due to the spin-reorientations of the domain wall. The existence of magnetic ordering was also confirmed by the AC magnetic susceptibility measurements of compound **2** performed at H_{dc} = 0 Oe and H_{ac} = 3.5 Oe at different frequencies (Figure S13). As can be seen from Figure S13, both $\chi_M{}'$ and $\chi_M{}''$ signals are frequency-independent, where the $\chi_M{}'$ signals show two peaks at ca. 14.8 K and 5.2 K with two corresponding non-zero $\chi_M{}''$ signals formed at temperatures below 16.2 and 6.2 K. The presence of $\chi_M{}'$ and $\chi_M{}''$ peaks at about 15 K are the result of the formation of an ordered state with an uncompensated moment and the peaks of $\chi_M{}'$ and $\chi_M{}''$ at about 5 K may be caused by spin-reforestation [62,63]. These data confirm the occurrence of magnetic ordering by weak ferromagnetism due to spin canting, which is consistent with the obtained results from ZFC/FC magnetizations data. Due to the presence of weak non-zero $\chi_M{}''$ signals, a coercive magnetic behavior would be expected below T_c.
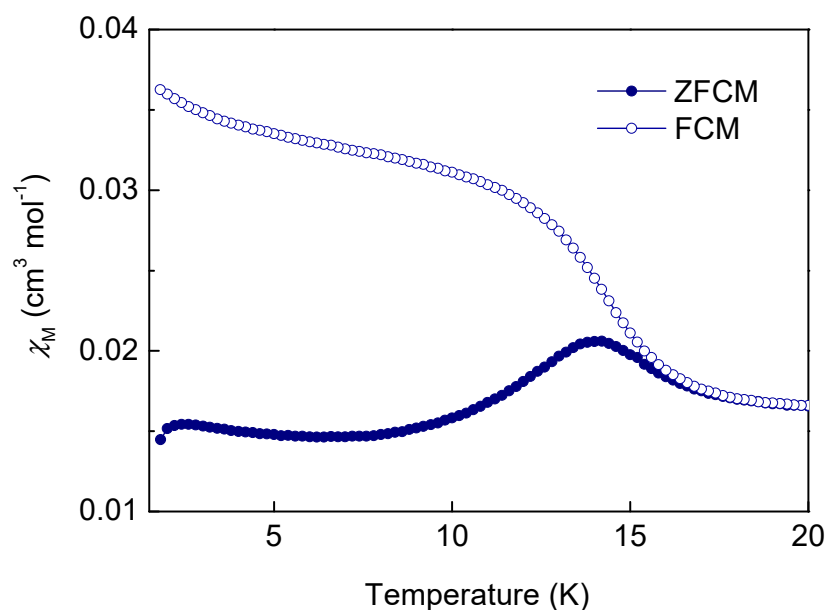
Figure 8. FC and ZFC magnetization plots of compound **2** at the field of 50 Oe.

To further study the magnetic ordering of compound **2**, the isothermal field-dependent magnetization was collected at 2.0 K. As depicted in Figure S14, the initial increase in magnetization shows a positive curvature to 0.175 $N\beta$ at 70 kOe, which is far below the theoretical value of saturation for an isotropic high-spin Co(II) system, and the absence of saturation of magnetization; this is an indication of an overall antiferromagnetic interaction between the Co(II) ions in compound **2**. In addition, when the field is less than 10 kOe, a hysteresis loop is clearly observed at 2.0 K, suggesting the soft magnet property of compound **2** (Figure S14, inset). The hysteresis loop shows a remanent magnetization (M_r) of $\approx$0.007 $N\beta$ and a coercive field of $\approx$350 Oe. Based on the value of M_r at 2.0 K, the canting angle of compound **2** is estimated to be approximately 0.20°, where M_S is 2.15 $N\beta$ for an octahedral Co(II) at 2 K with the effective spin of $S' = {}^1/_2$ and a common value of $g' = 4.3$ [60].

Finally, to rule out any contributions of Mn(II)/Mn(III) or Co(II) oxides in the low-temperature magnetic behaviors in compounds **1** and **2**, the AC magnetic data and 2.0 K field-dependent magnetization were collected using the thermal decomposed samples of **1** and **2** that had been heated at 350 °C for two hours (Figures S15–S18), in which the disappearance of peaks in χ_M' and/or χ_M'' and the absence of magnetic hysteresis loops in field-dependent magnetization are obtained, excluding the contribution of the behavior of Mn(II)/Mn(III) or Co(II) oxides.

3. Concluding Remarks

The results presented and discussed above have shown that the new compounds of general formula [M(N$_3$)$_2$(dmbpy)] for M = Mn (**1**) and Co (**2**) show very similar and almost identical linear chain structures, with alternating azide double bridging anions (EE and EO). Using magnetic studies down to a very low T (2K), the existence of intrachain ferro- and antiferromagnetic interactions was established, and these interactions are dominated by the double EE and double EO azido ligand bridges. Overall, the compounds are found to behave as antiferromagnets, and the study is relevant in the search for potentially cheap, stable and useful new magnets.

Compounds **1**·(Mn) and **2**·(Co) exhibit spin-canted antiferromagnetism at very low-temperatures, which is ascribed to the presence of single-ion anisotropy. Furthermore, below the Néel temperature, T_N, field-induced magnetic transitions have also been observed, and these are indicative for metamagnetism in the case of **1**·(Mn). Such coexistence of spin-canted antiferromagnetism and metamagnetism in 1D Mn(II) compounds with

alternating double EE and double EO azido ligands is unprecedented. Although the spin-canted antiferromagnetism might seem incompatible with the crystal structure of **2**, because of the presence of an inversion center between the bridged Mn(II) centers, the observation of the spin canting in **2** should be attributed to a structural phase transition, or a distortion in the crystal at low temperature, thereby removing the inversion center. Such types of distortions have been reported before [34,58]. The weak interchain interactions present in both compounds are ascribed to the π–π stacking interactions between the dmbpy rings.

4. Material and Methods

4.1. General Remarks

The starting materials (metal salts, sodium azide and the ligand 5,5'-dimethyl-2,2'-bipyridine, $C_{12}H_{12}N_2$), and used solvents were purchased from commercial sources (analytical reagent grade) and used without further purification. All the compounds were synthesized solvothermally under autogenous pressure. Azido derivatives are potentially explosive and should be handled with great care and prepared only in small quantities by trained persons.

4.2. Synthesis

Synthesis of catena-poly-[Mn(N$_3$)$_2$(dmbpy)] (**1**) A mixture of Mn(NO$_3$)$_2$ · 4H$_2$O (50 mg, 0.2 mmol), dmbpy (37 mg, 0.2 mmol) and NaN$_3$ (26 mg, 0.4 mmol) in H$_2$O/EtOH (3:1 *v/v*, 20 mL) was sealed in a Teflon-lined autoclave and heated at 130 °C for 2 days. After cooling to room temperature at a rate of 10 °C h^{-1}, yellow-colored crystals of **1** were obtained (yield 32%). Anal. Calcd. (%) for $C_{12}H_{12}MnN_8$: C, 44.59; H, 3.74; N, 34.67%. Found: C, 44.45; H, 3.92; N, 34.42%. Main IR band (KBr pellet, cm^{-1}): doublet at 2089s [ν(N$_3$$^-$)].

Synthesis of catena-poly-[Co(N$_3$)$_2$(dmbpy)] (**2**). This compound was prepared following a procedure similar to that of compound **1**, except that Co(NO$_3$)$_2$·6H$_2$O (58 mg, 0.2 mmol), was used instead of Mn(NO$_3$)$_2$·4H$_2$O. Brown-colored crystals were obtained, with a yield of 40%, containing **2**. Anal. Calcd. (%) for $C_{12}H_{12}CoN_8$: C, 44.05; H, 3.70; N, 34.24%. Found: C, 43.85; H, 3.82; N, 34.63%. Main IR band (KBr pellet, cm^{-1}): doublet at 2085s [ν(N$_3$$^-$)].

Physical Measurements. Elemental analyses of the obtained compounds (C, H and N) were performed using a Perkin–Elmer 2400 series II CHN analyzer. Infrared spectra were recorded as KBr pellets in the range 4000–400 cm^{-1} (4 cm^{-1} resolution) on a Perkin–Elmer 100 FT-IR spectrometer, which was calibrated using polystyrene and CO$_2$ bands. The temperature dependence DC and AC magnetic susceptibility measurements were performed on powdered samples, restrained in eicosane to prevent torquing, on a Quantum Design MPMS-7 SQUID (Superconducting Quantum Interference Device) and a PPMS (Physical Property Measurement System) magnetometer, equipped with 7.0 T and 9.0 T magnets (Quantum Design, San Diego, CA, USA), respectively, operated in the range of 2.0–300 K. Diamagnetic corrections were estimated from Pascal's constants [64] and subtracted from the experimental susceptibility data to obtain the molar paramagnetic susceptibility of the compounds. Powder X-ray diffraction (PXRD) measurements of **1** and **2** were carried out on a Siemens D-5000 diffractometer (Siemens, Karlsruhe, Germany) running in a step mode with a step size of 0.02° in θ and a fixed time of 10 s at 40 kV, 30 mA for Cu-Kα (λ = 1.5406 Å).

4.3. X-ray Crystallography

Diffraction data (Table 2) were collected at 200 K on a Bruker SMART X2S (Bruker AXS Inc., Madison, WI, USA) benchtop diffractometer [65], using the Mo *Kα* radiation (λ = 0.71073 Å) and the structures were refined with SHELXL [66,67]. Crystals for *M* = Co(II) were found to be twinned by a twofold rotation about the *c** reciprocal axis. One batch scale factor was refined, which converged to 0.24. All H atoms were placed in calculated positions and refined as riding to their carrier atoms.

Table 2. Crystal data and refinement parameters.

Compound/Deposition in CCDC	1/1954571	2/1954572
Formula	$C_{12}H_{12}MnN_8$	$C_{12}H_{12}CoN_8$
Fw	323.24	327.23
Crystal size (mm^3)	$0.5 \times 0.3 \times 0.2$	$0.30 \times 0.30 \times 0.18$
Space group	$P\text{-}1$	$P2_1/c$
a (Å)	7.8058(18)	7.397(2)
b (Å)	9.538(3)	18.373(4)
c (Å)	10.601(3)	10.661(3)
α (°)	113.630(8)	-
β (°)	102.610(8)	110.571(9)
γ (°)	93.223(8)	-
V ($Å^3$)	696.4(3)	1356.5(6)
Z, Z'	2, 1	4, 1
Diffractometer	Bruker X2S	Bruker X2S
Radiation	Mo-$K\alpha$	Mo-$K\alpha$
T (K)	200	200
Abs. coef. (mm^{-1})	0.954	1.272
Transmission fact.	0.56–0.83	0.51–0.80
Refl. collected	6450	8922
$\text{Sin}\theta/\lambda$ ($Å^{-1}$)	0.62	0.61
R_{int} (%)	4.26	8.68
Completeness (%)	97.4	99.2
Data/parameters	2658/192	2575/194
Restraints	0	0
R_1, wR_2 [$I > 2\sigma(I)$]	5.87, 16.64	6.53, 16.48
R_1, wR_2 [all data]	7.07, 17.60	8.26, 17.88
GOF on F^2	1.035	1.003

References

1. Khasainov, B.; Comet, M.; Veyssiere, B.; Spitzer, D. On the Mechanism of Efficiency of Lead Azide. *Propellants Explos. Pyrotech.* **2016**, *42*, 547–557. [CrossRef]
2. Xu, J.-G.; Sun, C.; Zhang, M.-J.; Liu, B.-W.; Li, X.-Z.; Lu, J.; Wang, S.-H.; Zheng, F.-K.; Guo, G.-C. Coordination Polymerization of Metal Azides and Powerful Nitrogen-Rich Ligand toward Primary Explosives with Excellent Energetic Performances. *Chem. Mater.* **2017**, *29*, 9725–9733. [CrossRef]
3. Ma, X.; Liu, Y.; Song, W.; Wang, Z.; Liu, X.; Xie, G.; Chen, S.; Gao, S. A difunctional azido-cobalt(ii) coordination polymer exhibiting slow magnetic relaxation behaviour and high-energy characteristics with good thermostability and insensitivity. *Dalton Trans.* **2018**, *47*, 12092–12104. [CrossRef] [PubMed]
4. Xu, J.-G.; Li, X.-Z.; Wu, H.-F.; Zheng, F.-K.; Chen, J.; Guo, G.-C. Substitution of Nitrogen-Rich Linkers with Insensitive Linkers in Azide-Based Energetic Coordination Polymers toward Safe Energetic Materials. *Cryst. Growth Des.* **2019**, *19*, 3934–3944. [CrossRef]
5. Zhang, W.; Li, T.; Zhang, B.; Wang, L.; Zhang, T.; Zhang, J. Planar, Energetic, π–π-Stacked Compound with Weak Interactions Resulting in a High-Impact- and Low-Friction-Sensitive, Safer, Primary Explosive. *Inorg. Chem.* **2019**, *58*, 7653–7656. [CrossRef]
6. Beck, W.; Werner, K.V. Reaktionen der Azido- und Isocyanatorhodium(I)-Komplexetrans-(Ph3P)2Rh(CO)X mit dem Nitrosyl-Kation in Gegenwart von Alkoholen. *Eur. J. Inorg. Chem.* **1973**, *106*, 868–873. [CrossRef]
7. Hu, B.-W.; Zhao, J.-P.; Yang, Q.; Liu, F.-C. Dzyaloshinski–Moriya (D–M) oriented weak ferromagnets in isomorphic coordination architectures constructed by flexible 1,2,4-triazole-1-acetate ligands with the assistance of halogen or pseudohalogen anions. *Inorg. Chem. Commun.* **2013**, *35*, 290–294. [CrossRef]
8. Ribas, J.; Escuer, A.; Monfort, M.; Vicente, R.; Cortés, R.; Lezama, L.; Rojo, T. Polynuclear NiII and MnII azido bridging complexes. Structural trends and magnetic behavior. *Coord. Chem. Rev.* **1999**, *193–195*, 1027–1068. [CrossRef]
9. Groom, C.R.; Bruno, I.J.; Lightfoot, M.P.; Ward, S.C. The Cambridge Structural Database. *Acta Crystallogr. Sect. B Struct. Sci. Cryst. Eng. Mater.* **2016**, *72*, 171–179. [CrossRef]
10. Ramírez, C.P.; Bernès, S.; Anzaldo, S.H.; Ortega, Y.R. Structure and NMR properties of the dinuclear complex di-μ-azido-κ4 N 1:N 1-bis[(azido-κN)(pyridine-2-carboxamide-κ2 N 1,O)zinc(II)]. *Acta Crystallogr. Sect. E Crystallogr. Commun.* **2021**, *77*, 111–116. [CrossRef]
11. Monfort, M.; Resino, I.; Ribas, J.; Solans, X.; Font-Bardia, M.; Rabu, P.; Drillon, M. Synthesis, structure, and magnetic properties of two new ferromagnetic/antiferromagnetic one-dimensional nickel(II) complexes. Magnetostructural correlations. *Inorg. Chem.* **2000**, *39*, 2572–2576. [CrossRef] [PubMed]
12. Monfort, M.; Resino, I.; Ribas, J.; Stoeckli-Evans, H. A Metamagnetic Two-Dimensional Molecular Material with Nickel(II) and Azide. *Angew. Chem. Int. Ed.* **2000**, *39*, 191–193. [CrossRef]
13. Cortés, R.; Drillon, M.; Solans, X.; Lezama, A.L.; Rojo, T. Alternating Ferromagnetic–Antiferromagnetic Interactions in a Manganese(II)–Azido One-Dimensional Compound: [Mn(bipy)(N3)2]. *Inorg. Chem.* **1997**, *36*, 677–683. [CrossRef]
14. Lu, Z.; Gamez, P.; Kou, H.-Z.; Fan, C.; Zhang, H.; Sun, G. Spin canting and metamagnetism in the two azido-bridged 1D complexes [Ni(3,5-dmpy)2(N3)2]n and [Co1.5(3,5-dmpy)3(N3)3]n. *CrystEngComm* **2012**, *14*, 5035–5041. [CrossRef]
15. Van Albada, G.A.; Van Der Horst, M.G.; Mutikainen, I.; Turpeinen, U.; Reedijk, J. Synthesis, Crystal Structure and Spectroscopy of catena-poly-bis(azido-N1,N1)(2-Aminopyrimidine)Copper(II). *J. Chem. Crystallogr.* **2008**, *38*, 413–417. [CrossRef]
16. Van Albada, G.A.; Van Der Horst, M.G.; Mutikainen, I.; Turpeinen, U.; Reedijk, J. Dinuclear and polynuclear Cu(II) azido-bridged compounds with 7-azaindole as a ligand. Synthesis, characterization and 3D structures. *Inorg. Chim. Acta* **2011**, *367*, 15–20. [CrossRef]
17. Van Albada, G.A.; Mutikainen, I.; Roubeau, O.; Reedijk, J. A dinuclear end-on azide-bridged copper(II) compound with weak antiferromagnetic interaction—Synthesis, characterization, magnetism and X-ray structure of bis[(μ-azido-κN1)-(azido-κN1)(1,3-bis(benzimidazol-2-yl)-2-methylpropane)copper(II)]. *J. Mol. Struct.* **2013**, *1036*, 252–256. [CrossRef]
18. Setifi, Z.; Ghazzali, M.; Glidewell, C.; Pérez, O.; Setifi, F.; Gómez-García, C.J.; Reedijk, J. Azide, water and adipate as bridging ligands for Cu(II): Synthesis, structure and magnetism of (μ4-adipato-κ-O)(μ-aqua)(μ-azido-κN1,N1)copper(II) monohydrate. *Polyhedron* **2016**, *117*, 244–248. [CrossRef]
19. Van Albada, G.A.; Mohamadou, A.; Mutikainen, I.; Turpeinen, U.; Reedijk, J. Diazidobis(2,2′-biimidazoline)nickel(II). *Acta Crystallogr. Sect. E Struct. Rep. Online* **2004**, *60*, m237–m238. [CrossRef]
20. Van Albada, G.A.; Smeets, W.J.J.; Spek, A.L.; Reedijk, J. The crystal structure and IR spectra of μ-(bipyrimidine-N1,N1′,N5,N5′)-bis[(azido-N1)(methanol)(bipyrimidine-N1,N1′)copper(II)] bis(triflate) bis(methanol). *J. Chem. Crystallogr.* **1998**, *28*, 427–432. [CrossRef]
21. Mautner, F.A.; Sudy, B.; Massoud, A.A.; Abu-Youssef, M.A.M. Synthesis and characterization of Mn(II) and Zn(II) azido complexes with halo-substituted pyridine derivative ligands. *Transit. Met. Chem.* **2013**, *38*, 319–325. [CrossRef]
22. Yue, Y.-F.; Gao, E.-Q.; Fang, C.-J.; Zheng, T.; Liang, J.; Yan, C.-H. Three Azido-Bridged Mn(II) Complexes Based on Open-Chain Diazine Schiff-base Ligands: Crystal Structures and Magnetic Properties. *Cryst. Growth Des.* **2008**, *8*, 3295–3301. [CrossRef]
23. Gao, E.-Q.; Bai, S.-Q.; Yue, Y.-F.; Wang, Z.-M.; Yan, C.-H. New One-Dimensional Azido-Bridged Manganese(II) Coordination Polymers Exhibiting Alternating Ferromagnetic–Antiferromagnetic Interactions: Structural and Magnetic Studies. *Inorg. Chem.* **2003**, *42*, 3642–3649. [CrossRef] [PubMed]

24. Abu-Youssef, M.A.M.; Drillon, M.; Escuer, A.; Goher, M.A.S.; Mautner, F.A.; Vicente, R. Topological Ferrimagnetic Behavior of Two New [Mn(L)2(N3)2]nChains with the New AF/AF/F Alternating Sequence (L = 3-Methylpyridine or 3,4-Dimethylpyridine). *Inorg. Chem.* **2000**, *39*, 5022–5027. [CrossRef] [PubMed]

25. Abu-Youssef, M.A.M.; Escuer, A.; Goher, M.A.S.; Mautner, F.A.; Reiss, G.J.; Vicente, R. Can a homometallic chain be ferromagnetic? *Angew. Chem. Int. Ed.* **2000**, *39*, 1624–1626. [CrossRef]

26. Ribas, J.; Monfort, M.; Ghosh, B.K.; Solans, X.; Font-Bardía, M. Versatility of the azido bridging ligand in the first two examples of ferro–antiferromagnetic alternating nickel(II) chains. *J. Chem. Soc. Chem. Commun.* **1995**, *23*, 2375–2376. [CrossRef]

27. Ribas, J.; Monfort, M.; Resino, I.; Solans, X.; Rabu, P.; Maingot, F.; Drillon, M. A Unique NiII Complex with Three Different Azido Bridges: Magneto-Structural Correlations in the First Triply Alternating *S* = 1 Chain. *Angew. Chem. Int. Ed.* **1996**, *35*, 2520–2522. [CrossRef]

28. Cortes, R.; Lezama, L.; Pizarro, J.L.; Arriortua, M.I.; Solans, X.; Rojo, T. Alternating Ferromagnetic and Antiferromagnetic Interactions In a MnII Chain With Alternating End-On and End-To-End Bridging Azido Ligands. *Angew. Chem. Int. Ed.* **1994**, *33*, 2488–2489. [CrossRef]

29. Viau, G.; Lombardi, M.G.; De Munno, G.; Julve, M.; Lloret, F.; Faus, J.; Caneschi, A.; Clemente-Juan, J.M. The azido ligand: A useful tool in designing chain compounds exhibiting alternating ferro- and antiferro-magnetic interactions. *Chem. Commun.* **1997**, *13*, 1195–1196. [CrossRef]

30. Alvarez, S.; Avnir, D.; Llunell, M.; Pinsky, M. Continuous symmetry maps and shape classification. The case of six-coordinated metal compounds. *New J. Chem.* **2002**, *26*, 996–1009. [CrossRef]

31. Bhowmik, P.; Biswas, S.; Chattopadhyay, S.; Diaz, C.; Gómez-García, C.J.; Ghosh, A. Synthesis, crystal structure and magnetic properties of two alternating double μ1,1 and μ1,3 azido bridged Cu(ii) and Ni(ii) chains. *Dalton Trans.* **2014**, *43*, 12414–12421. [CrossRef] [PubMed]

32. Wang, Y.-Q.; Tan, Q.-H.; Guo, X.-Y.; Liu, H.-T.; Liu, Z.-L.; Gao, E.-Q. Novel manganese(ii) and cobalt(ii) 2D polymers containing alternating chains with mixed azide and carboxylate bridges: Crystal structure and magnetic properties. *RSC Adv.* **2016**, *6*, 72326–72332. [CrossRef]

33. Fu, A.; Huang, X.; Li, J.; Yuen, T.; Lin, C.L. Controlled synthesis and magnetic properties of 2D and 3D iron azide networks infinity 2[Fe(N3)2(4,4′-bpy)] and infinity 3[Fe(N3)2(4,4′-bpy)]. *Chemistry* **2002**, *8*, 2239–2247. [CrossRef]

34. Zhang, J.-Y.; Liu, C.-M.; Zhang, D.-Q.; Gao, S.; Zhu, D.-B. Spin-canting in a 1D chain Mn(II) complex with alternating double end-on and double end-to-end azido bridging ligands. *Inorg. Chem. Commun.* **2007**, *10*, 897–901. [CrossRef]

35. Kar, P.; Drew, M.G.B.; Gómez-García, C.J.; Ghosh, A. Coordination Polymers Containing Manganese(II)-Azido Layers Connected by Dipyridyl-tetrazine and 4,4′-Azobis(pyridine) Linkers. *Inorg. Chem.* **2013**, *52*, 1640–1649. [CrossRef] [PubMed]

36. Mautner, F.A.; Berger, C.; Scherzer, M.; Fischer, R.C.; Maxwell, L.; Ruiz, E.; Vicente, R. Different topologies in three manganese-μ-azido 1D compounds: Magnetic behavior and DFT-quantum Monte Carlo calculations. *Dalton Trans.* **2015**, *44*, 18632–18642. [CrossRef] [PubMed]

37. Abu-Youssef, M.A.M.; Escuer, A.; Gatteschi, D.; Goher, M.A.S.; Mautner, F.A.; Vicente, R. Synthesis, Structural Characterization, Magnetic Behavior, and Single Crystal EPR Spectra of Three New One-Dimensional Manganese Azido Systems with FM, Alternating FM-AF, and AF Coupling. *Inorg. Chem.* **1999**, *38*, 5716–5723. [CrossRef]

38. Gao, E.-Q.; Cheng, A.-L.; Xu, Y.-X.; He, M.-Y.; Yan, C.-H. From Low-Dimensional Manganese(II) Azido Motifs to Higher-Dimensional Materials: Structure and Magnetic Properties. *Inorg. Chem.* **2005**, *44*, 8822–8835. [CrossRef]

39. Wang, X.-Y.; Wang, L.; Wang, Z.-M.; Su, G.; Gao, S. Coexistence of Spin-Canting, Metamagnetism, and Spin-Flop in a (4,4) Layered Manganese Azide Polymer. *Chem. Mater.* **2005**, *17*, 6369–6380. [CrossRef]

40. Zhang, X.-M.; Hao, Z.-M.; Zhang, W.-X.; Chen, X.-M. Dehydration-Induced Conversion from a Single-Chain Magnet into a Metamagnet in a Homometallic Nanoporous Metal–Organic Framework. *Angew. Chem. Int. Ed.* **2007**, *46*, 3456–3459. [CrossRef]

41. Cheng, X.-N.; Xue, W.; Huang, J.-H.; Chen, X.-M. Spin canting and/or metamagnetic behaviours of four isostructural grid-type coordination networks. *Dalton Trans.* **2009**, *29*, 5701–5707. [CrossRef] [PubMed]

42. Bellitto, C.; Federici, F.; Colapietro, M.; Portalone, G.; Caschera, D. X-ray Single-Crystal Structure and Magnetic Properties of Fe[CH3PO3)]·H2O: A Layered Weak Ferromagnet. *Inorg. Chem.* **2002**, *41*, 709–714. [CrossRef] [PubMed]

43. Liu, B.; Shang, R.; Hu, K.-L.; Wang, Z.-M.; Gao, S. A New Series of Chiral Metal Formate Frameworks of [HONH3][MII(HCOO)3] (M = Mn, Co, Ni, Zn, and Mg): Synthesis, Structures, and Properties. *Inorg. Chem.* **2012**, *51*, 13363–13372. [CrossRef] [PubMed]

44. Cheng, X.-N.; Xue, W.; Zhang, W.-X.; Chen, X.-M. Weak Ferromagnetism and Dynamic Magnetic Behavior of Two 2D Compounds with Hydroxy/Carboxylate-Bridged Co(II) Chains. *Chem. Mater.* **2008**, *20*, 5345–5350. [CrossRef]

45. Wang, T.-T.; Ren, M.; Bao, S.-S.; Liu, B.; Pi, L.; Cai, Z.-S.; Zheng, Z.-H.; Xu, Z.-L.; Zheng, L.-M. Effect of Structural Isomerism on Magnetic Dynamics: From Single-Molecule Magnet to Single-Chain Magnet. *Inorg. Chem.* **2014**, *53*, 3117–3125. [CrossRef]

46. Boca, R.; Herchel, R. Antisymmetric exchange in polynuclear metal complexes. *Coord. Chem. Rev.* **2010**, *254*, 2973–3025. [CrossRef]

47. Verdaguer, M.; Bleuzen, A.; Marvaud, V.; Vaissermann, J.; Seuleiman, M.; Desplanches, C.; Scuiller, A.; Train, C.; Garde, R.; Gelly, G.; et al. Molecules to build solids: High TC molecule-based magnets by design and recent revival of cyano complexes chemistry. *Coord. Chem. Rev.* **1999**, *190–192*, 1023–1047. [CrossRef]

48. Rodríguez, A.; Kivekäs, R.; Colacio, E. Unique self-assembled 2D metal-tetrazolate networks: Crystal structure and magnetic properties of [M(pmtz)2](M = Co(ii) and Fe(ii); Hpmtz = 5-(pyrimidyl)tetrazole). *Chem. Commun.* **2005**, *41*, 5228–5230. [CrossRef]

49. Li, J.-R.; Yu, Q.; Sañudo, E.C.; Tao, Y.; Bu, X.-H. An azido–CuII–triazolate complex with utp-type topological network, showing spin-canted antiferromagnetism. *Chem. Commun.* **2007**, *25*, 2602–2604. [CrossRef]

50. Wang, X.-Y.; Wei, H.-Y.; Wang, Z.-M.; Chen, Z.-D.; Gao, S. FormateThe Analogue of Azide: Structural and Magnetic Properties of M(HCOO)2(4,4′-bpy)·nH2O (M = Mn, Co, Ni; n = 0, 5). *Inorg. Chem.* **2005**, *44*, 572–583. [CrossRef]

51. Escuer, A.; Cano, J.; Goher, M.A.; Journaux, Y.; Lloret, F.; Mautner, F.A.; Vicente, R. Synthesis, Structural Characterization, and Monte Carlo Simulation of the Magnetic Properties of Two New Alternating MnIIAzide 2-D Honeycombs. Study of the Ferromagnetic Ordered Phase below 20 K. *Inorg. Chem.* **2000**, *39*, 4688–4695. [CrossRef] [PubMed]

52. Cheng, L.; Zhang, W.-X.; Ye, B.-H.; Lin, J.-B.; Chen, X.-M. Spin Canting and Topological Ferrimagnetism in Two Manganese(II) Coordination Polymers Generated by In Situ Solvothermal Ligand Reactions. *Eur. J. Inorg. Chem.* **2007**, *2007*, 2668–2676. [CrossRef]

53. Carlin, R.L.; Van Duyneveldt, A.J. Field-dependent magnetic phenomena. *Acc. Chem. Res.* **1980**, *13*, 231–236. [CrossRef]

54. Manson, J.L.; Kmety, C.R.; Palacio, F.; Epstein, A.J.; Miller, J.S. Low-Field Remanent Magnetization in the Weak Ferromagnet Mn[N(CN)2]2. Evidence for Spin-Flop Behavior. *Chem. Mater.* **2001**, *13*, 1068–1073. [CrossRef]

55. Pinkowicz, D.; Rams, M.; Nitek, W.; Czarnecki, B.; Sieklucka, B. Evidence for magnetic anisotropy of [NbIV(CN)8]4– in a pillared-layered Mn2Nb framework showing spin-flop transition. *Chem. Commun.* **2012**, *48*, 8323–8325. [CrossRef]

56. Lu, Y.-B.; Wang, M.-S.; Zhou, W.-W.; Xu, G.; Guo, G.-C.; Huang, J.-S. Novel 3-D PtS-like Tetrazolate-Bridged Manganese(II) Complex Exhibiting Spin-Canted Antiferromagnetism and Field-Induced Spin-Flop Transition. *Inorg. Chem.* **2008**, *47*, 8935–8942. [CrossRef] [PubMed]

57. Schlueter, J.A.; Manson, J.L.; Hyzer, K.A.; Geiser, U. Spin Canting in the 3D Anionic Dicyanamide Structure (SPh3)Mn(dca)3(Ph = Phenyl, dca = Dicyanamide). *Inorg. Chem.* **2004**, *43*, 4100–4102. [CrossRef]

58. Ray, U.; Jasimuddin, S.; Ghosh, B.K.; Monfort, M.; Ribas, J.; Mostafa, G.; Lu, T.-H.; Sinha, C. A New Alternating Ferro-Antiferromagnetic One-Dimensional Azido-Bridged (Arylazoimidazole)manganese(II), [Mn(TaiEt)(N3)2]n [TaiEt = 1-Ethyl-2-(p-tolylazo)imidazole], Exhibiting Bulk Weak Ferromagnetic Long-Range Ordering. *Eur. J. Inorg. Chem.* **2004**, *2004*, 250–259. [CrossRef]

59. Boonmak, J.; Nakano, M.; Youngme, S. Structural diversity and magnetic properties in 1D and 2D azido-bridged cobalt(ii) complexes with 1,2-bis(2-pyridyl)ethylene. *Dalton Trans.* **2011**, *40*, 1254–1260. [CrossRef]

60. Boonmak, J.; Nakano, M.; Chaichit, N.; Pakawatchai, C.; Youngme, S. Spin Canting and Metamagnetism in 2D and 3D Cobalt(II) Coordination Networks with Alternating Double End-On and Double End-to-End Azido Bridges. *Inorg. Chem.* **2011**, *50*, 7324–7333. [CrossRef]

61. Wang, X.-T.; Wang, X.-H.; Wang, Z.-M.; Gao, S. Diversity of Azido Magnetic Chains Constructed with Flexible Ligand 2,2′-Dipyridylamine. *Inorg. Chem.* **2009**, *48*, 1301–1308. [CrossRef] [PubMed]

62. Li, R.-Y.; Wang, X.-Y.; Liu, T.; Xu, H.-B.; Zhao, F.; Wang, Z.-M.; Gao, S. Synthesis, Structure, and Magnetism of Three Azido-Bridged Co2+Compounds with a Flexible Coligand 1,2-(Tetrazole-1-yl)ethane. *Inorg. Chem.* **2008**, *47*, 8134–8142. [CrossRef] [PubMed]

63. Bałanda, M. AC Susceptibility Studies of Phase Transitions and Magnetic Relaxation: Conventional, Molecular and Low-Dimensional Magnets. *Acta Phys. Pol. A* **2013**, *124*, 964–976. [CrossRef]

64. Bain, G.A.; Berry, J.F. Diamagnetic Corrections and Pascal's Constants. *J. Chem. Educ.* **2008**, *85*, 532–533. [CrossRef]

65. Eccles, K.S.; Stokes, S.P.; Daly, C.A.; Barry, N.M.; McSweeney, S.P.; O'Neill, D.J.; Kelly, D.M.; Jennings, W.B.; Dhubhghaill, O.M.N.; Moynihan, H.A.; et al. Evaluation of the Bruker SMART X2S: Crystallography for the nonspecialist? *J. Appl. Crystallogr.* **2010**, *44*, 213–215. [CrossRef]

66. Sheldrick, G.M. A short history of SHELX. *Acta Crystallogr. A* **2008**, *64*, 112–122. [CrossRef]

67. Sheldrick, G.M. Crystal structure refinement with SHELXL. *Acta Crystallogr.* **2015**, *71*, 3–8. [CrossRef]